On the vehicle state estimation benefits of smart tires

V. Mazzilli[1,2], D. Ivone[3], V. Vidal Muñoz[1,4], S. De Pinto[2] , P. Camocardi[2], L. Pascali[2], A. Doria Cerezo[4], P. Gruber[1], G. Tarquinio[2], A. Sorniotti[1]

[1] University of Surrey, Guildford, GU2 7XH, UK
[2] McLaren Automotive Ltd, Woking, GU21 4YH, UK
[3] Pirelli & C. S.p.A., 20126 Milan, IT
[4] Universidad Politécnica de Cataluña, Barcelona, 08034, SPA

Abstract. Smart tires are systems that are able to measure temperature, inflation pressure, footprint dimensions, and, importantly, tire contact forces. The integration of this additional information with the signals obtained from more conventional vehicle sensors, e.g., inertial measurement units, can enhance state estimation in production cars. This paper evaluates the use of smart tires to improve the estimation performance of an Unscented Kalman filter (UKF) based on a nonlinear vehicle dynamics model. Two UKF implementations, excluding and including smart tire information, are compared in terms of estimation accuracy of vehicle speed, sideslip angle and tire-road friction coefficient, using experimental data obtained on a high performance passenger car.

Keywords. Sideslip angle estimation, vehicle speed estimation, tire-road friction coefficient estimation, smart tire system.

1 Introduction

Modern vehicle dynamics controllers are improved by adding more information about vehicle states. The inputs from multiple sources are processed by state estimators to predict vehicle variables that are not easily measurable, such as the sideslip angle at the center of gravity, and the vehicle speed during high tire slip ratio conditions. The recent literature mostly adopts estimation algorithms based on Kalman filters using dynamic models of the vehicle. Despite the good accuracy provided by Extended Kalman filters, nowadays Unscented Kalman filters (UKFs) are widely adopted for their superior robustness with respect to sampling rates and approximation errors, for the same computational effort [1]. UKFs have also been proven to be effective in estimating vehicle parameters, in addition to vehicle motion states, see [2]–[4].

A common feature of the available model based state estimation implementations is to consider the tire as a passive component; the tire-road interaction is usually described by numerical models, which present significant inaccuracies and parameter dependencies that can affect the quality of the estimation. In this context, the introduction of tire sensing systems ([5], [6]) offers the possibility of adding a direct feedback contribution to enhance state estimation robustness with respect to the inaccuracies of the tire force models. These solutions open promising scenarios in terms of vehicle state estimation

and control system development, see [7]– [10].

This paper addresses the benefits of the integration of smart tires in a dynamic model based state estimator, by experimentally comparing two UKF algorithms, including and excluding the information from a smart tire system, during extreme handling maneuvers. The points of novelty are:

- The implementation of smart tire technologies developed by Pirelli, namely the Cyber^{TM} Tyre system, in a high performance passenger car;
- The design of a novel Cyber^{TM} Tyre based UKF, i.e., the UKF-CT, which includes the Cyber^{TM} Tyre signals as feedback contribution in the measurement update phase of the filter;
- The optimization of the estimator parameters to achieve a fair comparison between the two considered estimator designs, including and excluding the Cyber^{TM} Tyre inputs;
- The objective evaluation of the resulting vehicle speed and sideslip angle estimation, together with the road condition factor as additional filter parameter;
- The analysis of the enhanced estimation performance and robustness associated with the longitudinal and vertical tire force information on each vehicle corner, provided by the Cyber^{TM} Tyre system.

The paper is organized as follows: Section 2 is an overview on Cyber^{TM} Tyre system technology; Section 3 describes the state estimation architecture; finally, Section 4 describes the tuning procedure, and shows the comparison results between the UKF-CT and a state-of-the art estimator not using the Cyber^{TM} Tyre inputs, which is referred to as UKF in the remainder.

2 Cyber^{TM} Tyre system technology

In vehicle dynamics, one of the most promising innovations is to use the tires as sensing systems to provide useful information to the vehicle controllers. In fact, the tire is in a very privileged position being the only part of the vehicle that is in contact with the road. The smart tire concept refers to a tire equipped with sensors and digital computing systems for monitoring thermal and mechanical parameters that may be shared with the vehicle control units while driving. The possibility of measuring important variables directly from the tires offers the potential for significantly improving the performances of existing active control systems, and developing new control strategies for enhanced safety and efficiency.

Pirelli Tyre S.p.A. is proposing technologies for embedding sensors in the inner liner of the tire, to make the tire itself an active element of the vehicle. The adopted sensors are tiny and light, and have minimal impact on the production process. They have a wide bandwidth, high reliability, and the robustness required to resist the impulses occurring when the sensor enters and exits the footprint. The Cyber^{TM} Tyre project has the main purpose of developing an innovative sensor able to measure the relevant variables through a tri-axial accelerometer, to condition the signals, and to transmit them to a receiver located on the vehicle. Another crucial aspect is the elaboration of the collected signals during the tire rolling motion, by adopting ad-hoc algorithms to extract useful information.

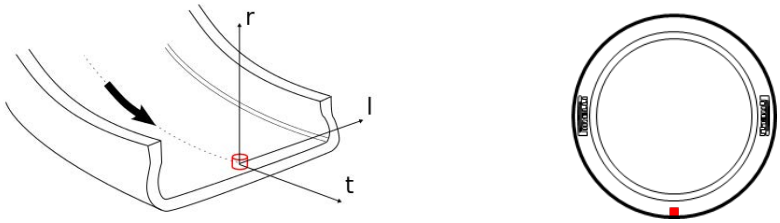

Fig. 1. Sensor reference frame: radial (r), tangential (t) and lateral (l) axes [7].

Among the available Cyber™ Tyre features, this study uses the normal and longitudinal tire force information that is provided once per wheel rotation, as each tire has one sensor placed on the inner liner, as shown in Fig. 1. The generation of these quantities requires specific algorithms developed through preliminary indoor calibration tests, where the extrapolation of relevant parameters is possible in controlled environment.

The Cyber™ Tyre system capability of estimating the normal and longitudinal contact forces is shown in Fig. 2, during a portion of an experimental vehicle test in a handling scenario involving considerable longitudinal and lateral accelerations. The comparison between the forces measured by a commercial dynamometric hub and the corresponding values from the Cyber™ Tyre system highlights the smart tire ability to provide reliable estimation of the contact forces.

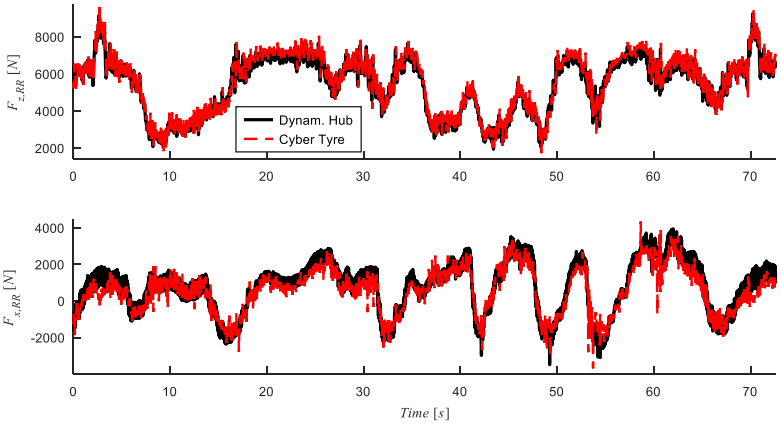

Fig. 2. Comparison between the vertical and longitudinal forces on the rear right wheel, respectively $F_{z,RR}$ and $F_{x,RR}$, measured by a dynamometric hub and generated by the Cyber™ Tyre system during a typical handling maneuver.

3 State estimation architecture

This section describes the vehicle model embedded in the proposed UKF, and the UKF algorithms for state and parameter estimation.

3.1 Vehicle model

The UKF implementations of this study use a 7-degree-of-freedom (7DOF) planar two-track model of the case study rear-wheel-drive high performance passenger car, which considers the longitudinal, lateral and yaw dynamics of the vehicle, as well as the wheel dynamics. The heave and pitch dynamics are not included, whilst the roll angle is considered statically dependent on the lateral acceleration and suspension characteristics.

Fig. 3 shows the vehicle schematic, with positive directions of the vectors, according to the ISO convention [11]. In the following formulations, the subscript i, with $i = F, R$, indicates the axle, while the subscript j, with $j = L, R$, indicates the vehicle side. In the figure, V is the vehicle velocity, having longitudinal and lateral components v_x and v_y; β is the sideslip angle; $F_{x,ij}$ and $F_{y,ij}$ are the longitudinal and lateral tire forces; δ_{Fj} is the steering angle at the front wheels; $\dot{\psi}$ is the vehicle yaw rate; t_i is the track width; and l_i is the longitudinal distance between the center of gravity and the axle. In addition to the steering angle, the model inputs are the engine and braking torque values, M_{ICE} and $M_{B,ij}$.

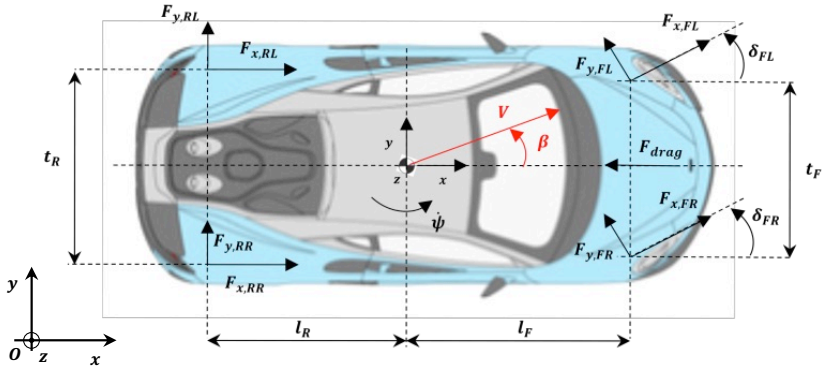

Fig. 3. Vehicle schematic with indication of the main parameters and variables.

The longitudinal force balance equation is:

$$a_x = \dot{v}_x - \dot{\psi} v_y = \frac{1}{m}\left[\sum_{j=L}^{R}(F_{x,Fj}\cos\delta_{Fj} - F_{y,Fj}\sin\delta_{Fj}) + \sum_{j=L}^{R} F_{x,Rj} - F_{drag}\right] \quad (1)$$

where a_x is the longitudinal acceleration, m is the vehicle mass, and F_{drag} is the aerodynamic drag force. The lateral force balance equation is:

$$a_y = \dot{v}_y + \dot{\psi} v_x = \frac{1}{m}\left[\sum_{j=L}^{R}(F_{x,Fj}\sin\delta_{Fj} + F_{y,Fj}\cos\delta_{Fj}) + \sum_{j=L}^{R} F_{y,Rj}\right] \quad (2)$$

where a_y is the lateral acceleration. The yaw moment balance equation is:

$$\ddot{\psi} = \frac{1}{J_z}\Bigg[l_F \sum_{j=L}^{R} \left(F_{x,Fj} sin\delta_{Fj} + F_{y,Fj} cos\delta_{Fj}\right) - l_R \sum_{j=L}^{R} F_{y,Rj} - \frac{t_F}{2}\left(F_{x,FL}\cos\delta_{FL} - F_{x,FR}\cos\delta_{FR}\right) + \frac{t_F}{2}\left(F_{y,FL}\sin\delta_{FL} - F_{y,FR}\sin\delta_{FR}\right) - \frac{t_R}{2}\left(F_{x,RL} - F_{x,RR}\right) + \sum M_{z,ij}\Bigg] \tag{3}$$

where $M_{z,ij}$ is the self-aligning moment of the tires. The vehicle speed and sideslip angle are given by:

$$V = \sqrt{v_x^2 + v_y^2}\,; \quad \beta = \tan^{-1}\left(\frac{v_y}{v_x}\right) \tag{4}$$

The Pacejka Magic Formula 2002 calculates the rolling radius, laden radius, rolling resistance, longitudinal force, lateral force, and aligning moment of the tires, namely $R_{e,ij}$, $R_{l,ij}$, $M_{y,ij}$, $F_{x,ij}$, $F_{y,ij}$ and $M_{z,ij}$, as functions of the slip angle α_{ij}, longitudinal slip ratio $\sigma_{x,ij}$, vertical load $F_{z,ij}$, and camber angle γ_{ij}, which depends on the static roll angle. The tire slip ratio formulation resembles the one in [12]:

$$\sigma_{x,ij} = \frac{\omega_{ij} R_{e,ij} - V_{w_{x,ij}}}{\max\left(\left|V_{w_{x,ij}}\right|, \eta v_{x,marg}\right)} \tag{5}$$

where $V_{w_{x,ij}}$ is the longitudinal component of the peripheral wheel speed; ω_{ij} is the angular wheel speed; $v_{x,marg}$ is the marginal speed, namely the minimum speed ensuring system stability when the vehicle model reaches a low speed; and $\eta = 1.1$ is a safety coefficient. This formulation facilitates the removal of the wheel speed oscillations at very low speed, which are typical numerical issues of the conventional slip ratio formulations.

The calculation of the vertical tire loads on each corner, $F_{z,ij}$, includes consideration of the longitudinal and lateral load transfers and aerodynamic downforce contributions. The lateral load transfers are evaluated in static conditions, considering the lateral acceleration and roll moment distribution between the front and rear axles.

Each wheel dynamics are described by a moment balance equation, which, for the rear wheels, is:

$$J_{w_{eq,Rj}} \dot{\omega}_{Rj} = 0.5\, M_{ICE} i_{tr} \eta_{tr} - M_{B,Rj} - F_{x,Rj} R_{l,Rj} - M_{y,Rj} \tag{6}$$

where $J_{w_{eq,Rj}}$ is the equivalent mass moment of inertia of the wheel, including the powertrain inertia; i_{tr} is the transmission gear ratio; and η_{tr} is the transmission efficiency.

3.2 Unscented Kalman filter

The UKF ([1], [13]) is an iterative algorithm including: i) a time update step, in which the set of nonlinear equations describing the process are subject to forward Euler integration; and ii) a measurement update step, in which the data from the available sensors are used to estimate the n states of the system [14].

Within the UKF algorithm, the nonlinear model of Section 3.1 is re-arranged as:

$$\begin{cases} x_k = f(x_{k-1}, u_k, w_{k-1}) \\ y_k = h(x_k, u_k, v_k) \end{cases} \tag{7}$$

where f describes the system dynamics; h is the measurement model; $x_k \in \mathbb{R}^n$ is the state vector at the time step k, assumed to have Gaussian probability distribution $P_k \in \mathbb{R}^n$; $u_k \in \mathbb{R}^r$ and $y_k \in \mathbb{R}^m$ are the input and output vectors; and the random variables $w_{k-1} \in \mathbb{R}^n$ and $v_k \in \mathbb{R}^m$ are the process and measurement noise vectors. The noise vectors are assumed to be uncorrelated with zero-mean Gaussian probability distributions $Q \in \mathbb{R}^{n \times n}$ and $R \in \mathbb{R}^{m \times m}$.

To avoid neglecting any odd-moment information, the UKF algorithm uses an augmented state vector, x_{aug}, with size $N = 2n + m$, and the corresponding augmented error system covariance matrix, P_{aug}, see [1], [2]:

$$x_{aug} = \{x_{k-1} \;\; w_{k-1} \;\; v_k\}^T ; \quad P_{aug} = \begin{bmatrix} P_{k-1} & 0 & 0 \\ 0 & Q & 0 \\ 0 & 0 & R \end{bmatrix} \tag{8}$$

As the noise components are uncorrelated, the covariance matrices are diagonal. Ideally, Q and R should change at each iteration because the uncertainties related to the process and sensors might vary. However, unlike P_{k-1}, Q and R are kept constant to reduce the computational load, and aid the estimation of the error covariance P_k and the Kalman gain K_k to quickly converge and stabilize [14].

3.3 Parameter estimation

In vehicle dynamics, the main issue of the model based state estimation approach is its strong dependency on varying vehicle parameters, i.e., vehicle mass, center of gravity position, and tire parameters, including the tire-road friction coefficient. In particular, tire parameter accuracy is crucial in determining the contact forces. In [13], parameter estimation is accomplished by extending the augmented state vector with a new state-space representation during the time update step. The new state, i.e., the estimated parameter, is described by a random walk model, a stationary process only driven by the corresponding process noise.

In this study, similarly to [7], the estimated parameter is the road condition factor, μ_{max}. Its dynamics are described by:

$$\dot{\mu}_{max} = 0 \rightarrow \mu_{max,k} = \mu_{max,k-1} + w_{\mu_{max},k-1} \tag{9}$$

where $w_{\mu_{max},k-1}$ is the associated process noise. This factor constitutes an additional degree of freedom, increasing the vehicle model robustness by scaling the tire-road friction coefficient in the Pacejka tire model formulation [2].

3.4 Unscented Kalman filter implementation

Fig. 4 shows the schematic of the UKF-CT implementation, including the Cyber^{TM} Tyre measurements. The main objective of the UKF-CT is to obtain the values of the most relevant vehicle states, i.e., the vehicle sideslip angle at the center of gravity, β, and the vehicle speed, V, for a wide range of operating conditions. The state and input vectors resemble those of the UKF described in [2], which was implemented on a real

car by Bosch. The output vector includes the variables that are available on the controller area network (CAN) bus of the vehicle, see [3], [4]. Moreover, due to the availability of the estimated longitudinal tire forces, $F_{x,ij}$, and vertical loads, $F_{z,ij}$, output by the Cyber^{TM} Tyre system, the vector y is augmented accordingly. Hence, the resulting vectors are:

$$\begin{gathered} x = \{v_x \quad v_y \quad \dot{\psi} \quad \omega_{ij} \quad \mu_{max}\} \\ u = \{\delta_{Fj} \quad M_{ICE} \quad M_{B,ij}\} \\ y_{UKF} = \{a_x \quad a_y \quad \dot{\psi} \quad \omega_{ij}\} \\ y_{UKF-CT} = \{y_{UKF} \quad F_{z,ij} \quad F_{x,ij}\} \end{gathered} \tag{10}$$

where the subscripts UKF and $UKF - CT$, used here and in the remainder, refer to the estimators excluding and including the smart tire system estimations. The angular wheel speeds, ω_{ij}, allow the estimation of vehicle speed; the additional measurement of a_x, not included the implementation in [2], helps prevent performance degradation in conditions of significant longitudinal tire slip ratios.

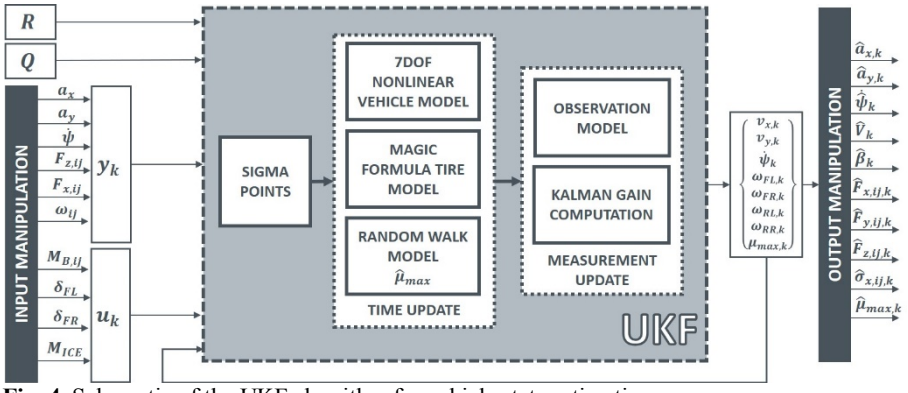

Fig. 4. Schematic of the UKF algorithm for vehicle state estimation.

The measurement noise covariance R, i.e., the variance of the sensors, was determined through the a-priori analysis of sample measurements [14], whilst the matrix Q is a tuning parameter that takes model uncertainties into account. To reduce the number of tuning parameters, the initial error system covariance matrix is set to be equal to Q, as in [4]. The additional parameters are α_{UT}, a constant defining the spread of the sigma points, which is set to 1 in the proposed implementations; β_{UT}, a constant related to the type of probability distribution, equal to 2 for Gaussian distribution; and κ_{UT}, a scaling parameter, set to 1 [1].

4 Results

This section deals with the experimental comparison of the UKF and UKF-CT, and the analysis of the improvements deriving from the addition of the Cyber^{TM} Tyre force outputs. The experimental activity was performed on a McLaren 570s equipped with sensorized Pirelli P Zero Corsa tires, as well as an OxTS RT unit and a 6D IMU, to

directly measure the sideslip angle at the center of gravity, vehicle speed, and longitudinal and lateral accelerations.

The two filters were tuned through the optimization routine described in Section 4.1, and are compared by using the experimental measurements acquired during track tests covering a wide range of driving scenarios. The signals to perform the measurement updates within the filters are those available on the CAN bus of the vehicle, whilst the acquired signals from the OxTS RT unit and 6D IMU are used as reference to check the estimation performance.

4.1 Tuning routine

The filter tuning routine uses an optimization process to find the values of the diagonal elements of Q for both filters. The rationale is to obtain two sets of covariances, one for the UKF and one for the UKF-CT, which minimize optimality criteria, to achieve an objective comparison of the estimation performance.

Due to the complexity and important nonlinearities, a multi-objective genetic algorithm has been selected, minimizing three objective functions based on the root mean square error ($RMSE$) between: i) the data acquired from the OxTS RT unit and 6D IMU, in a portion of a handling circuit in dry conditions; and ii) the estimation outputs, obtained by feeding the filters with the required CAN bus signals during the same training maneuver.

The values of the three functions are normalized to build a 3D Pareto frontier. The selected optimum refers to the set of covariances corresponding to the closest point of the Pareto frontier to the origin of the 3D system. The optimization problem is defined as:

$$\begin{aligned}
&\min_{\arg Q} J_\beta \quad s.t. \quad Q_i \in [Q_{i,min}, Q_{i,max}], \quad J_\beta = \sqrt{\frac{1}{N_s}\sum_{i=1}^{N_s}\left(\beta - \hat{\beta}\right)^2} \\
&\min_{\arg Q} J_{a_x} \quad s.t. \quad Q_i \in [Q_{i,min}, Q_{i,max}], \quad J_{a_x} = \sqrt{\frac{1}{N_s}\sum_{i=1}^{N_s}(a_x - \hat{a}_x)^2} \\
&\min_{\arg Q} J_{a_y} \quad s.t. \quad Q_i \in [Q_{i,min}, Q_{i,max}], \quad J_{a_y} = \sqrt{\frac{1}{N_s}\sum_{i=1}^{N_s}\left(a_y - \hat{a}_y\right)^2}
\end{aligned} \tag{11}$$

where J_β, J_{a_x} and J_{a_y} are the objective functions, considering the tracking performance in terms of sideslip angle, longitudinal acceleration, and lateral acceleration; N_s is the number of samples; $Q_{i,min}$ and $Q_{i,max}$ define the range of variation of each element Q_i of Q; and the estimated quantities are indicated with '^'.

The state vector is initialized as:

$$x_0 = \{0.95V \quad 0 \quad 0 \quad 0.95\omega_{FL} \quad 0.95\omega_{FR} \quad 0.95\omega_{RL} \quad 0.95\omega_{RR} \quad 0.7\} \tag{12}$$

where the initial vehicle and wheel speeds are 95% of the acquired CAN signals. The initial conditions for β and $\dot{\psi}$ are set to 0, as the vehicle usually starts from a straight

trajectory. Moreover, by considering an initial road condition factor of 0.7, the estimator is brought relatively far from the ideal scenario in terms of speed and parameter estimation, and thus the optimization also tends to improve the convergence features of the estimator.

The optimal covariances computed for the specific dry handling scenario were used to obtain the results in the following sections.

4.2 Selected maneuvers and key performance indicators

The selected maneuvers for state estimation performance comparison are:

- Handling circuit lap in dry conditions. Note that this is a different dataset from the one used for the definition of the optimal covariances in Section 4.1;
- Handling circuit lap in wet conditions, to analyze how the estimators perform in low-grip scenarios;
- Open-loop step steer [15], to evaluate the response of the estimators during extreme cornering transients.

Four key performance indicators (KPIs) are defined for an objective comparison:

- The root mean square value of the estimation error for the considered states:

$$RMSE = \sqrt{\frac{1}{N_s}\sum_{i=1}^{N_s}\left(Y - \hat{Y}\right)^2} \tag{13}$$

where Y is the real measurement, and $\hat{Y}$ is the corresponding estimated value;

- The difference (in percentage) between $RMSE_{UKF-CT}$ and $RMSE_{UKF}$:

$$\Delta RMSE_{\%} = \frac{RMSE_{UKF-CT} - RMSE_{UKF}}{RMSE_{UKF}} 100 \tag{14}$$

- The maximum absolute value of the estimation error:

$$e^{max} = max\left|Y - \hat{Y}\right| \tag{15}$$

- The difference (in percentage) between e^{max}_{UKF-CT} and e^{max}_{UKF}:

$$\Delta e^{max}_{\%} = \frac{e^{max}_{UKF-CT} - e^{max}_{UKF}}{e^{max}_{UKF}} 100 \tag{16}$$

4.3 Handling circuit lap in dry conditions

The estimation results along a portion of a race track in dry conditions are shown in Fig. 5, while the KPIs are reported in Table 1. The initial μ_{max} was set to 1.1, typical value for the dry tarmac of a vehicle proving ground, see [16].

Both filters provide good performance, with the UKF-CT showing lower $RMSE$ values on the main estimated quantities. The vehicle speed estimation is in line with the target, set by the involved car maker, of not exceeding a $RMSE$ value of 3% of the top speed, with maximum error values of 4.9 km/h and 3.3 km/h for the UKF and UKF-CT. Furthermore, for both estimators, the maximum sideslip angle estimation error remains within the limits mentioned by Grip et al. [16], i.e., within ~1 deg, which allows effective operation of active chassis controllers.

The profiles of the road condition factor are rather steady at reasonable levels for both estimators, even though they converge to different values in the second half of the test, i.e., μ_{max} marginally increases for the UKF, and decreases for the UKF-CT. This kind of difference is normal, and is caused by the fact that the algorithms modify μ_{max} to improve the convergence and overall estimation, since the road condition factor dynamics are not described by a formulation based on the physics of the system, but they are only modeled as process noise [2]. Nevertheless, in the UKF-CT, μ_{max} can be considered closer to the real road condition. In fact, once the road condition factor of the UKF-CT varies, the β estimate matches the measurement very well. On the contrary, in the same condition, the UKF underestimates $|\beta|$, and therefore its μ_{max} can be considered overestimated. The conclusion is that the parameter estimation is enhanced by the additional contribution of the tire forces also in nominal dry tarmac scenarios, close to the one adopted for tuning the estimators. This causes the better sideslip angle estimation performance of the UKF-CT.

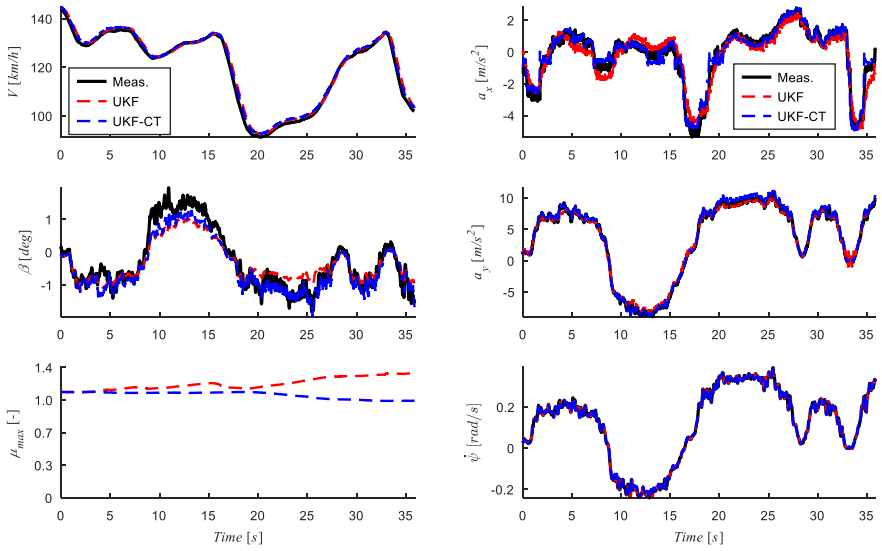

Fig. 5. Estimation results in a handling circuit lap in dry conditions.

Table 1. KPIs for a handling circuit lap in dry conditions.

Variable	Unit	$RMSE_{UKF}$	$RMSE_{UKF-CT}$	$\Delta RMSE_{\%}$	e_{UKF}^{max}	e_{UKF-CT}^{max}	$\Delta e_{\%}^{max}$
V	[km/h]	1.749	1.256	-28.17%	4.910	3.328	-32.22%
β	[deg]	0.363	0.293	-19.34%	1.070	0.957	-10.58%
$\dot{\psi}$	[rad/s]	0.003	0.006	98.36%	0.012	0.029	135.84%
a_x	[m/s^2]	0.526	0.390	-25.76%	2.277	2.790	22.50%
a_y	[m/s^2]	0.433	0.369	-14.80%	1.623	1.176	-27.54%

4.4 Handling circuit lap in wet conditions

The second scenario is a track lap with wet tarmac, in which μ_{max} is expected to be ranging from 0.5 to 0.7. The maneuver was selected to analyze filter robustness when the vehicle operates in low-grip conditions and at high $|\beta|$ values, reaching a maximum of 20 deg (Fig. 6). The initial condition for the estimated μ_{max} was purposely set to 1, to check the estimation convergence.

In such extreme handling conditions, the tire model approximations can lead to inaccuracies that increase the process uncertainty. To cope with this criticality, previous literature implemented adaptive strategies to vary the covariances whenever the process or sensors become unreliable due to the driving conditions [17]. However, as the scope of this research is to analyze the robustness improvements caused by the $F_{x,ij}$ and $F_{z,ij}$ measurements, the filter calibration was kept the same as for the dry handling maneuver.

In Fig. 6, the UKF shows greater oscillation peaks in the a_x and a_y profiles, caused by the overestimation of the road condition factor, which, in the UKF-CT, converges more promptly and to the correct value. Overall, the UKF-CT provides better performance, and is reliable also during the high slip ratio conditions occurring in the time window ~17-19 s, when the vehicle is subject to hard braking after a swift acceleration. Here, the UKF reaches the maximum speed estimation error, due to the loss of reliability of the angular wheel speed signals.

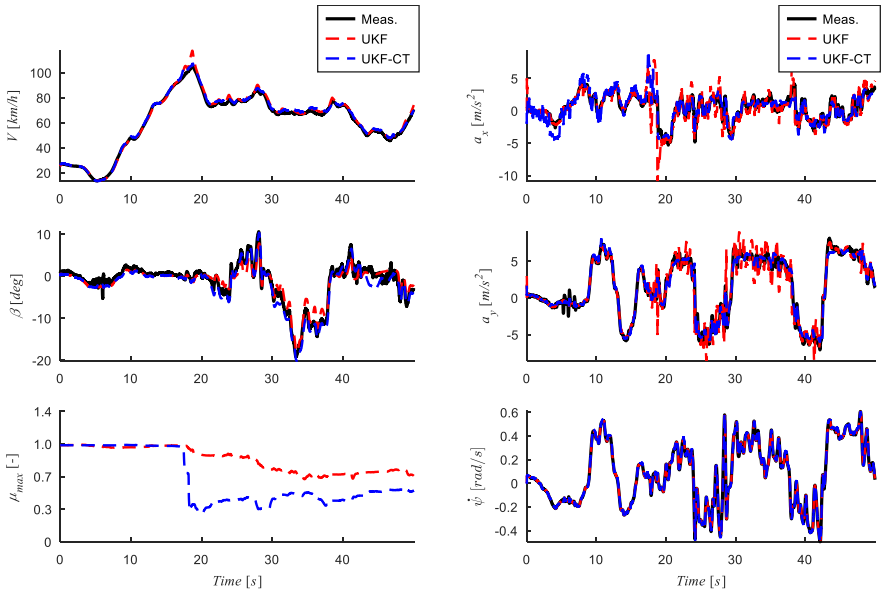

Fig. 6. Estimation results in a handling circuit lap in wet conditions.

In Table 2, the $RMSE_{UKF-CT}$ of the vehicle speed is approximately 1.5 km/h, which corresponds to a -33% $\Delta RMSE_{\%}$. The superiority of the UKF-CT is also noticeable in the sideslip angle estimation, with a $\Delta RMSE_{\%}$ of -11%, and in the longitudinal and lateral accelerations, with $\Delta RMSE_{\%}$ equal to -21.5% and -49%. These estimation errors

make the UKF-CT suitable for feedback control applications in large sideslip conditions. In terms of yaw rate, in all considered scenarios the UKF-CT generates higher errors than the UKF; nonetheless, these do not cause concern, as they have limited values with respect to the nature of the maneuver.

Table 2. KPIs for a handling circuit lap in wet conditions.

Variable	Unit	$RMSE_{UKF}$	$RMSE_{UKF-CT}$	$\Delta RMSE_{\%}$	e_{UKF}^{max}	e_{UKF-CT}^{max}	$\Delta e_{\%}^{max}$
V	[km/h]	2.187	1.462	-33.14%	12.946	5.484	-57.64%
β	[deg]	1.397	1.239	-11.28%	4.220	4.715	11.74%
$\dot{\psi}$	[rad/s]	0.007	0.015	110.10%	0.068	0.143	109.35%
a_x	[m/s^2]	1.241	0.974	-21.52%	12.170	7.592	-37.62%
a_y	[m/s^2]	1.055	0.538	-49.02%	8.155	3.069	-62.37%

4.5 Open-loop step steer (ISO 7401, [15])

The last maneuver, i.e., a step steep in dry conditions, allows to evaluate the estimation performance during an extreme cornering transient. The maneuver consists of a first steering wheel angle step with a 100 deg amplitude, followed by an abrupt countersteering action. The initial value of μ_{max} was purposely set to 0.7, which is different from the actual value for the specific experimental scenario.

Grip et al. [16] discussed that when the vehicle is in steady-state conditions, the μ_{max} estimation does not have enough excitation to converge to its final value. Therefore, in this test, the road condition parameter remains constant (Fig. 7) until the step steering input is applied. Fig. 7 shows that the UKF-CT is significantly faster than the UKF in adapting μ_{max}. In fact, the UKF-CT takes 0.72 s to reach 95% of the final μ_{max} value, whilst the UKF takes 2.76 s. This means that the a_x and a_y estimates from the UKF are slower in matching the experimental peak values. For this reason, some authors, such as Piyabongkarn et al. [18], fuse the dynamic model based estimation with the output of kinematic models that are independent from vehicle and tire parameters, and can provide fast state estimation response during transients. However, the important conclusion of this analysis is that good and robust performance in extreme transient conditions can be achieved through the tire force contribution of the UKF-CT, without the addition of any cascade of estimators or adaptive algorithms.

Table 3 shows that the $RMSE$ values for the sideslip angle and the acceleration components are ~30% to ~50% lower for the UKF-CT. On the other hand, the vehicle speed estimation performance is comparable, and the yaw rate trend is well described in both cases, even if the error is smaller for the UKF.

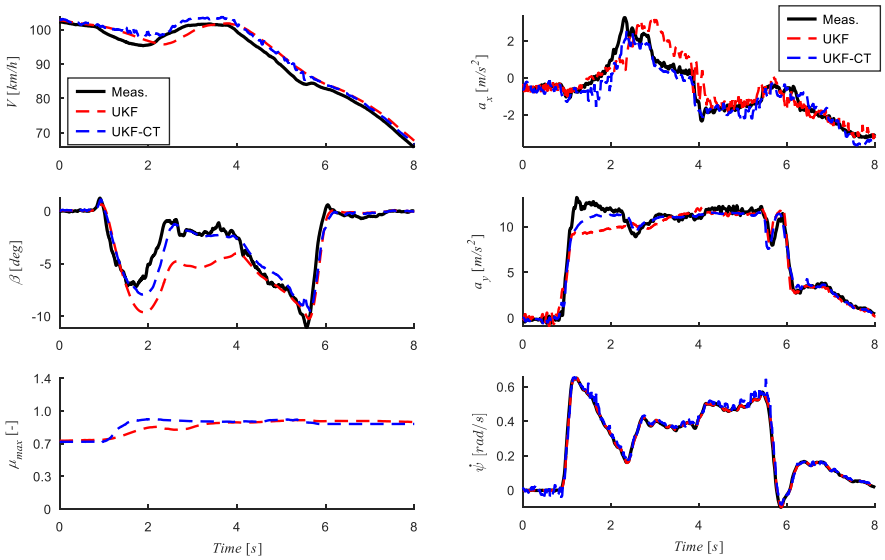

Fig. 7. Estimation results in a step steer maneuver in dry conditions.

Table 3. KPIs for a step steer maneuver in dry conditions.

Variable	Unit	$RMSE_{UKF}$	$RMSE_{UKF-CT}$	$\Delta RMSE_{\%}$	e_{UKF}^{max}	e_{UKF-CT}^{max}	$\Delta e_{\%}^{max}$
V	[km/h]	2.009	1.947	-3.08%	3.733	4.563	22.24%
β	[deg]	2.004	0.916	-54.29%	5.413	2.912	-46.20%
$\dot{\psi}$	[rad/s]	0.007	0.021	184.06%	0.040	0.120	198.66%
a_x	[m/s^2]	0.711	0.430	-39.51%	2.723	1.547	-43.18%
a_y	[m/s^2]	1.161	0.711	-38.76%	3.566	2.783	-21.97%

Conclusions

The paper described a novel estimator, the UKF-CT, of the key dynamic states for vehicle dynamics control, and discussed a selection of intermediate results in the context of an extensive activity focused on a high performance passenger car. The main feature of the UKF-CT is the inclusion in the measurement vector of the longitudinal and vertical tire forces from the Cyber™ Tyre system.

The performance of the UKF-CT was compared with that of a state-of-the-art estimator, i.e., a UKF not using the Cyber™ Tyre system inputs, during extreme handling maneuvers with different tire-road friction conditions, carried out with a McLaren 570s. For fairness of comparison, the estimators were tuned through an optimization routine based on a genetic algorithm, to find the process covariances minimizing the estimation errors during dry tarmac operation. The covariances were then kept constant for the evaluation.

The experimental results show that the tire force feedback improves the robustness of the estimation and the speed of the adaptation to different road conditions. As a result, the UKF-CT implementation improves the estimation accuracy of the vehicle states, even during extreme transients and in low friction conditions.

Future developments will explore robust tuning methods and adaptive implementations of the process covariances, and involve experimental testing along a wider range of driving scenarios.

References

[1] E. A. Wan and R. Van Der Merwe, "The unscented Kalman filter for nonlinear estimation," *Adapt. Syst. Signal Process. Commun. Control Symp.*, 2000.

[2] S. Antonov, A. Fehn, and A. Kugi, "Unscented Kalman filter for vehicle state estimation," *Veh. Syst. Dyn.*, vol. 49, no. 9, pp. 1497–1520, 2011.

[3] H. Heidfeld, M. Schünemann, and R. Kasper, "UKF-based state and tire slip estimation for a 4WD electric vehicle," *Veh. Syst. Dyn.*, pp. 1–18, 2019 (in press).

[4] M. Wielitzka, A. Busch, M. Dagen, and T. Ortmaier, "Unscented Kalman Filter for State and Parameter Estimation in Vehicle Dynamics," *Kalman Filters - Theory Adv. Appl.*, In Tech, pp. 56–75, 2018.

[5] F. Braghin, M. Brusarosco, F. Cheli, A. Cigada, S. Manzoni, and F. Mancosu, "Measurement of contact forces and patch features by means of accelerometers fixed inside the tire to improve future car active control," *Veh. Syst. Dyn.*, vol. 44, Issue sup1, pp. 3–13, 2006.

[6] S. C. Ergen, A. Sangiovanni-Vincentelli, X. Sun, R. Tebano, S. Alalusi, G. Audisio, and M. Sabatini, "The tire as an intelligent sensor," *IEEE Trans. Comput. Des. Integr. Circ. Syst.*, vol. 28, no. 7, pp. 941–955, 2009.

[7] E. Sabbioni, D. Ivone, F. Braghin, and F. Cheli, "In-tyre sensors induced benefits on sideslip angle and friction coefficient estimation," *SAE Tech. Pap. 2015-01-1510*, 2015.

[8] K. B. Singh and S. Taheri, "Estimation of tire–road friction coefficient and its application in chassis control systems," *Syst. Sci. Control Eng.*, vol. 3, no. 1, pp. 39–61, 2015.

[9] F. Cheli, E. Leo, S. Melzi, and E. Sabbioni, "On the impact of 'smart tyres' on existing ABS/EBD control systems," *Veh. Syst. Dyn.*, vol. 48, Issue sup1, pp. 255–270, 2010.

[10] K. B. Singh, M. A. Arat, and S. Taheri, "Literature review and fundamental approaches for vehicle and tire state estimation," *Veh. Syst. Dyn.*, vol. 57, no. 11, pp. 1643–1665, 2019.

[11] "Road vehicles – Vehicle dynamics and road-holding ability – Vocabulary," *BS ISO 8855*, pp. 1–52, 2011.

[12] T. Y. Kim, S. Jung, and W. S. Yoo, "Advanced slip ratio for ensuring numerical stability of low-speed driving simulation: Part I – longitudinal slip ratio," *Proc. Inst. Mech. Eng. Part D J. Automob. Eng.*, vol. 233, no. 8, pp. 2000-2006, 2019.

[13] S. Haykin, *Kalman Filtering and Neural Networks*, John Wiley & Sons, 2001.

[14] G. Welch and G. Bishop, “An Introduction to the Kalman Filter,” SIGGRAPH, pp. 19–33, 2001.
[15] “Road vehicles – Lateral transient response test methods – Open-loop test methods,” *ISO 74012011(E)*, pp. 1–67, 2011.
[16] H. F. Grip, L. Imsland, T. Johansen, J. C. Kalkkuhl, and A. Suissa, “Vehicle Sideslip Estimation: Design, Implementation, and Experimental Validation,” *IEEE Control Syst. Mag.*, vol. 29, no. 5, pp. 36–52, 2009.
[17] L. Li, G. Jia, X. Ran, J. Song, and K. Wu, “A variable structure extended Kalman filter for vehicle sideslip angle estimation on a low friction road,” *Veh. Syst. Dyn.*, vol. 52, no. 2, pp. 280–308, 2014.
[18] D. Piyabongkarn, R. Rajamani, J. A. Grogg, and J. Y. Lew, “Development and experimental evaluation of a slip angle estimator for vehicle stability control,” *IEEE Trans. Control Syst. Technol.*, vol. 17, no. 1, pp. 78–88, 2009.